

## Quantum scattering, resonant states, and conductance fluctuations in an open square electron billiard

I. V. Zozoulenko and K.-F. Berggren

*Department of Physics and Measurement Technology, Linköping University, S-581 83 Linköping, Sweden*

(Received 5 March 1997; revised manuscript received 15 April 1997)

Electron transport was studied in an open square quantum dot with a dimension typical for current experiments. A numerical analysis of the probability density distribution inside the dot was performed which enabled us to unambiguously map the resonant states which dominate the conductance of the structure. It was shown that, despite the presence of dot openings, transport through the dot is effectively mediated by just a few (or even a single) eigenstates of the corresponding closed structure. In a single-mode regime in the leads, the broadening of the resonant levels is typically smaller than the mean energy level spacing,  $\Delta$ . On the contrary, in the many-mode regime this broadening typically exceeds  $\Delta$  and has an irregular, essentially non-Lorentzian, character. It was demonstrated that in the latter case eigenlevel spacing statistics of the corresponding closed system are not relevant to the averaged transport properties of the dot. This conclusion seems to have a number of experimental as well as numerical verifications. The calculated periodicity of the conduction oscillations in the open dot is related to the formation of the global shell structure of the corresponding isolated square. The shell structure reflects periodic clustering of levels on the scale exceeding the mean level spacing separation. Each shell can be ascribed to the certain family of the periodic orbits in the square. However, a particular arrangement of the leads may lead to the selective coupling between them, so that not all shells (or, alternatively, families of periodic orbits) mediate transport through the dot. This selective coupling leading to the suppression of the contribution from some families of orbits can be tested experimentally on the dots with the different arrangements of the leads. [S0163-1829(97)04535-9]

### I. INTRODUCTION

In nanoscaled semiconductor quantum dots, electron motion is confined in all spatial dimensions and the lateral shape of the dot can be controlled by an applied gate voltage.<sup>1-12</sup> In high quality samples at low temperatures, the phase coherence length often well exceeds the dimension of the device and large-angle elastic scattering events occur only at the boundaries of the structure. Such a transport regime is usually referred to as ballistic. During recent years a great deal of effort has been focused on the transport properties of ballistic microstructures. In particular, the statistical properties of the conductance fluctuations of quantum dots have received great attention, both theoretically<sup>13-21</sup> and experimentally.<sup>1-9</sup> Due to their reduced size, ballistic dots represent rewarding objects for studying the relation between quantum mechanics and the corresponding semiclassical electron dynamics. This reveals itself in the geometry-specific, nonaveraged features in the conductance fluctuations.<sup>1,6,8-12,19-24</sup>

For interpreting the magnetoconductance oscillations in a circular quantum dot, a simple "shell structure" (or "tunneling") model has been put forward by Persson *et al.*<sup>6</sup> It relates the conductance fluctuations to the density of states (DOS) of the corresponding closed system. The DOS is characterized by the global shell structure which reflects a periodic clustering of levels on the scale exceeding the mean level spacing separation. The DOS of the isolated dot is assumed to be Lorentzian broadened due to the effects of lead openings and it is calculated on the basis of the Gutzwiller periodic orbit theory<sup>23</sup> or quantum mechanically.<sup>6,24</sup> This

model is well-justified for noninteracting systems in a tunneling regime of the weak coupling to the leads. It has been argued, however, that it can be used when the leads become open. The correspondence between magnetoconductance oscillations and the oscillatory character of the DOS has also been found in antidot arrays.<sup>25</sup> In addition, shell structures which have been detected experimentally in the spectra of small metal clusters, have been successfully interpreted in terms of the periodic orbit theory for the DOS.<sup>26</sup>

Our present work is motivated in part, by a recent experiment,<sup>11,12</sup> where highly periodic conductance oscillations have been found in the zero-field resistance of the ballistic square dot as the Fermi wave vector,  $k_F$ , was varied. Here we critically examine the shell-structure model for the square dot. We compare predictions given by this model to the quantum mechanical calculations performed for the open square geometry with the dimension typical for real structures. We show that the calculated periodicity of the conduction oscillations in the open dot is related to the formation of the global shell structure in the DOS of the corresponding isolated square. There exists a certain correspondence between the character of eigenstates defining different shells and the related families of periodic orbits. We also demonstrate that particular arrangements of the leads may lead to a selective coupling such that only selected shells (or, alternatively, periodic orbits) effectively mediate transport through the dot.

The second motivation of our work stems from the current interest in the highly topical area of "quantum chaos."<sup>27</sup> The statistics of the nearest level spacing in classically non-integrable chaotic billiards in the absence of a magnetic field obeys the Wigner or Gaussian orthogonal en-

semble distribution. This is usually taken as a definition of quantum chaos, which is a quantum mechanical analog to classical chaotic dynamics in a closed billiard. In contrast, for classically regular systems the corresponding statistics is Poisson-like, which reflects an integrable character of the underlying classical dynamics. Transport properties of open systems are often analyzed on the basis of the level spacing statistics of the corresponding isolated dots. This is not an *a priori* evident assumption and several conflicting reports do exist in the literature on the effects of leads on the electron dynamics in open systems. In particular, Ref. 28 shows that the statistics of the spectra for open dots (which are defined in terms of the dwell time) are exactly the same as those of the corresponding closed system. At the same time, results<sup>20,29</sup> suggest that the leads attached to the dot may change the level statistics, so that transition to chaos can occur in a nominally regular system. On the contrary, Wang *et al.*<sup>30</sup> conclude that the openness of the dot makes chaotic scattering nonessential.

Besides, in the current literature one can find a broad spectrum of opinions on the possibility of resolving, in the transport experiment on the open dot, resonant states related to the eigenlevels of corresponding isolated structure. (When the dot becomes open, eigenlevels interact and acquire a finite broadening due to the finite lifetime associated with the possibility for electrons to escape from the dot via leads.) In the many-mode regime in the leads, this broadening might well exceed the mean energy level separation,  $\Delta$ , resulting in an overlap of a vast number of resonances. Also, the presence of dot openings may cause a significant distortion of corresponding eigenstates. Under these circumstances it is not clear whether a discussion of transport through an open dot on the basis of the properties of the closed structure is still meaningful. To the best of our knowledge, up to now no direct theoretical calculations on the actual broadening of the resonant levels for the open dots in the transmissive regime are available.

In this paper we hope to contribute to the clarification of the above mentioned issues. Our numerical analysis enables us to unambiguously map the resonant states mediating transport through the open square and to find their broadening. We demonstrate, that despite the openness, transport through the dot takes place via just a few resonant energy states. In a single-mode regime the broadening of the resonant levels is typically smaller than  $\Delta$ . As far as the single-mode regime is concerned, our results tend to support the conclusion<sup>28</sup> that the statistics of the spectra for open dots follows that one of the corresponding closed system. However, in the many-mode regime, energy broadening typically exceeds  $\Delta$  and has an irregular, essentially non-Lorentzian character. We demonstrate that in this case eigenlevel spacing statistics of the corresponding closed system are not relevant to the averaged transport properties of the dot. This conclusion seems to have a number of experimental as well as numerical verifications.

The paper is organized as follows. In Sec. II we present the basic theory which we use for our calculations of the dot conductance and the mapping of resonant states mediating the transport in the dot. In Sec. III we discuss resonant states of the open dot. We focus on the three different transport regimes, namely, the tunneling, the single-mode, and the

many-mode regimes. In this section we also examine ‘‘scarred’’ features seen in the wave-function pattern in the transmissive regime. Finally, we critically examine the possibility of discussing transport characteristics of open dots on the basis of the eigenlevel spacing statistics of the corresponding isolated systems. In Sec. IV we review the ‘‘shell-structure’’ model of conductance oscillations for the square dot and compare it with our full quantum mechanical calculations. A summary of the main results of Sec. V concludes the paper. A very preliminary account on a part of this work has been presented previously.<sup>12</sup>

## II. BASIC THEORY

The system under investigation is a relatively large square dot with the side  $L = 1 \mu\text{m}$  which is typical for current experiments. It is connected to reservoirs<sup>31</sup> by quantum-point-contact- (QPC-) like openings (leads). While the dimension of the square is fixed, the arrangement and number of leads are varied as will be depicted in the insets to the figures. In the present work we concentrate mostly on the transport through open dots, such that Coulomb charging is not important. For the sake of simplicity, hard wall confinement and a flat potential profile inside the dot are assumed which seems to be a good approximation for large dots.<sup>23,32</sup> We disregard effects of the soft impurity potential due to remote donors. Recent theoretical studies show that the influence of this potential on quantum transport in the dots appears to play only a minor role.<sup>33,34</sup> As we focus on the ballistic regime of transport when the phase coherence length,  $l_\phi$ , exceeds the dimension of the dot,  $L$ , inelastic scattering is disregarded. We briefly discuss effects of the inelastic scattering on the conductance through the dot in Sec. IV.

Our calculations are based on the Landauer-Büttiker formalism which relates the conductance properties of the device to its scattering characteristics.<sup>35</sup> In the simplest case of the two-terminal geometry zero-temperature conductance reads  $G(\epsilon, T=0) = 2e^2/h \text{Tr}(\mathbf{t}\mathbf{t}^\dagger)$ , where  $t_{\alpha,\beta}(\epsilon) = (\mathbf{t})_{\alpha,\beta}$  is the transmission amplitude from incoming state  $\alpha$  to outgoing state  $\beta$  at energy  $\epsilon$ . The effects of a finite temperature are accounted for by the convolution of  $G(\epsilon, 0)$  with the derivative of the Fermi-Dirac distribution,  $f(E_F, T)$ , at the given Fermi energy,  $E_F$ ,  $G(E_F, T) = -\int d\epsilon G(\epsilon, 0) \partial f(\epsilon - E_F, T) / \partial \epsilon$ .<sup>35</sup> The scattering matrix  $\mathbf{t}$  is calculated on the basis of a hybrid recursive Green-function technique<sup>36</sup> which is proven to be numerically efficient, in particular, for the case of large structures and high magnetic fields.

In order to understand the relations between the conductance fluctuations and resonant energy states of the square, we study the probability density distribution inside the dot,  $\Psi(x, y)$ . A drawback of the Green function technique used here is that one does not obtain the wave function everywhere in the system after the scattering problem is solved. Thus, to calculate  $\Psi(x, y)$  we first solve a scattering problem and find the Green functions in the inner (dot+openings) region and transmission and reflection amplitudes (and, therefore, wave functions) at the boundary slices between the inner region and the reservoirs (i.e., wide leads). Then, recursively iterating slice by slice inside the dot by making use of the Dyson equation, we recover  $\Psi(x, y)$  in the inner region. Details of the calculations are reported elsewhere.<sup>37</sup>

Analyzing the probability density distribution inside the dot we are in a position to identify resonant energy states which effectively mediate transport through the dot at a given  $E_F$ . To do this, we numerically expand the solution of the scattering problem in the open dot,  $\Psi(x,y;E)$ , in the set of eigenstates of the closed dot,  $\psi_{mn} = (2/L)\sin(\pi mx/L)\sin(\pi ny/L)$  [with eigenenergies  $\epsilon_{mn} = \hbar^2/2m^*(k_m^2 + k_n^2)$ ;  $k_m = (\pi m/L)$ ,  $k_n = (\pi n/L)$ ]

$$\Psi(x,y;E) = \frac{2}{L} \sum_m \sum_n c_{mn}(E) \sin \frac{\pi mx}{L} \sin \frac{\pi ny}{L}. \quad (1)$$

To outline the meaning of the expansion coefficients  $c_{mn}$  we start from the trivial case of an isolated dot. In this situation the wave function in the left hand side of Eq. (1) is one of the eigenstates of the system, such that  $c_{mn}(E) = \delta_{E,\epsilon_{mn}}$  represent discrete eigenlevel spectrum of the dot. When the system becomes open, the time which electron spends in the dot becomes finite. Therefore, eigenenergy levels acquire a finite broadening and transform into *resonant states*. Obviously, coefficients  $c_{mn}$  represent the contributions of the resonant states  $\{m,n\}$  (associated with the corresponding eigenstates  $\{m,n\}$ ) in the total wave function. An energy interval where  $|c_{mn}(E)|^2$  is distinct from zero gives a broadening of the resonant state  $\{m,n\}$ . With further opening of the dot, the scattering state becomes a linear combination of the individual broadened states  $\{m,n\}$ .

Similar mapping of the resonant states of the open dot can be performed for a structure of arbitrary shape and with a finite magnetic field applied. In this case, generally, one has to start from the numerical solution of eigenvalue problem calculating a complete set of eigenstates. This would make a corresponding numerical analysis much more complicated and time consuming. For the square geometry, Eq. (1) is simply equivalent to the complex space sine-Fourier transform. Therefore, we can use standard fast numerical methods for performing such a transform which greatly facilitates our calculations. Note, that a similar analysis based on the space sine-Fourier transform expansion of the experimentally observed ‘‘scarlets’’ pattern in the water surface driven by the high-frequency shaker in tanks with different shapes has been done in Ref. 38.

### III. RESONANT STATES OF THE SQUARE DOT

#### A. Tunneling regime

In this section we discuss the relations between resonant eigenstates of the dot and conductance peaks in the tunneling regime, when the dot is weakly coupled to the leads (see inset in Fig. 1). In what follows we consider an idealized model of noninteracting electrons.

Each conductance peak, as shown in Fig. 1, corresponds to an excitation of one single resonant energy level which effectively mediates transport at the given Fermi energy. Near its maximum, each peak is characterized by the Lorentzian shape, in accordance to the Breit-Wigner formalism<sup>39</sup> (this can be seen on the scale much finer than that one of Fig. 1). The positions of the peaks are shifted with respect to the corresponding eigenenergy levels of the isolated square [cf. Figs. 1(a) and 1(b)]. Because of the presence of the tunneling barriers of the finite height, the wave function in the dot is

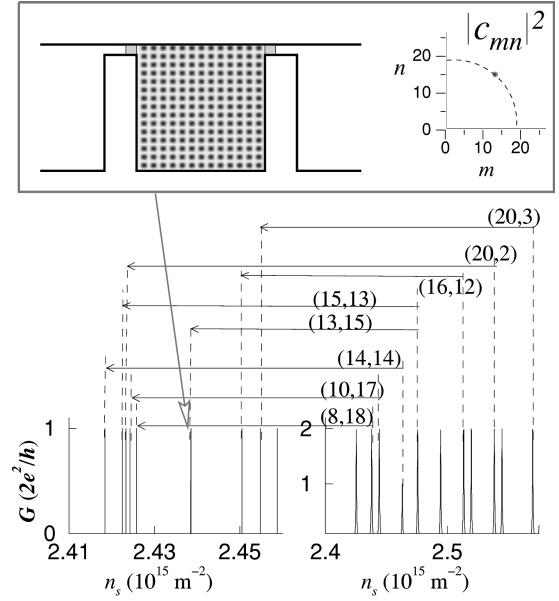


FIG. 1. Lower left: The conductance of the square dot (schematically depicted in the upper panel) in the tunneling regime as a function of the sheet electron density  $n_s = E_F m^* / \pi \hbar^2$ . Temperature  $T=0$ . Shadow regions in the leads represent tunneling barriers with the height exceeding the Fermi energy. Lower right: Eigenenergy levels of the isolated dot. Height of the peaks represents the degree of degeneracy (1 or 2). Upper panel shows the calculated probability density distribution  $|\Psi(x,y)|^2$  inside the dot for one of the tunneling peaks (left) and the corresponding numerical results for the coefficients  $|c_{mn}|^2$  calculated on the basis of Eq. (1) (right). Dashed lines indicate the circle with the radius  $r = k_F L / \pi$ . A similar analysis has been done for the rest of the peaks and the correspondence between eigenstates of the isolated square and resonant levels of the dot is indicated by the arrows. Quantum numbers of the resonant states,  $(m,n)$ , are shown in the parenthesis. In the case under consideration the side of the dot was chosen to be  $L = 0.5 \mu\text{m}$  (in contrast to the case of open dots, Figs. 2–5, where  $L = 1 \mu\text{m}$ .)

somewhat extended into the barrier region. Thus, in the present arrangement of the leads, the  $x$  component of the wave vector is always smaller than the corresponding value for the isolated dot,  $k_m = \pi m/L$ . The larger the quantum number  $m$ , the more the wave function extends into the tunneling barrier region. This lifts a level degeneracy and causes the shifting of the positions of resonant level maxima towards lower energies in comparison to the unperturbed dot. As an example, see Fig. 1, a double degenerate level  $(13,15), (15,13)$  of the isolated dot splits, with a larger shift for the state  $(15,13)$  which has larger quantum number  $m$ . A shifting of resonant levels was also found in the case of tunneling through a T-shaped nanostructure whose size was comparable to the Fermi wavelength.<sup>40</sup>

#### B. Single-mode regime

Figure 2(a) shows conductance fluctuations of the open square dot where lead openings are adjusted to support one propagating mode. The probability density distribution  $|\Psi_{mn}|^2$  is shown for two representative values of the Fermi wave vector,  $k_F = \sqrt{2m^* E_F / \hbar} = \sqrt{2\pi n_s}$ , where  $n_s$  is the sheet electron density. Here the pattern of  $|\Psi(x,y)|^2$  exhibits a complicated structure, where eigenstates of the isolated

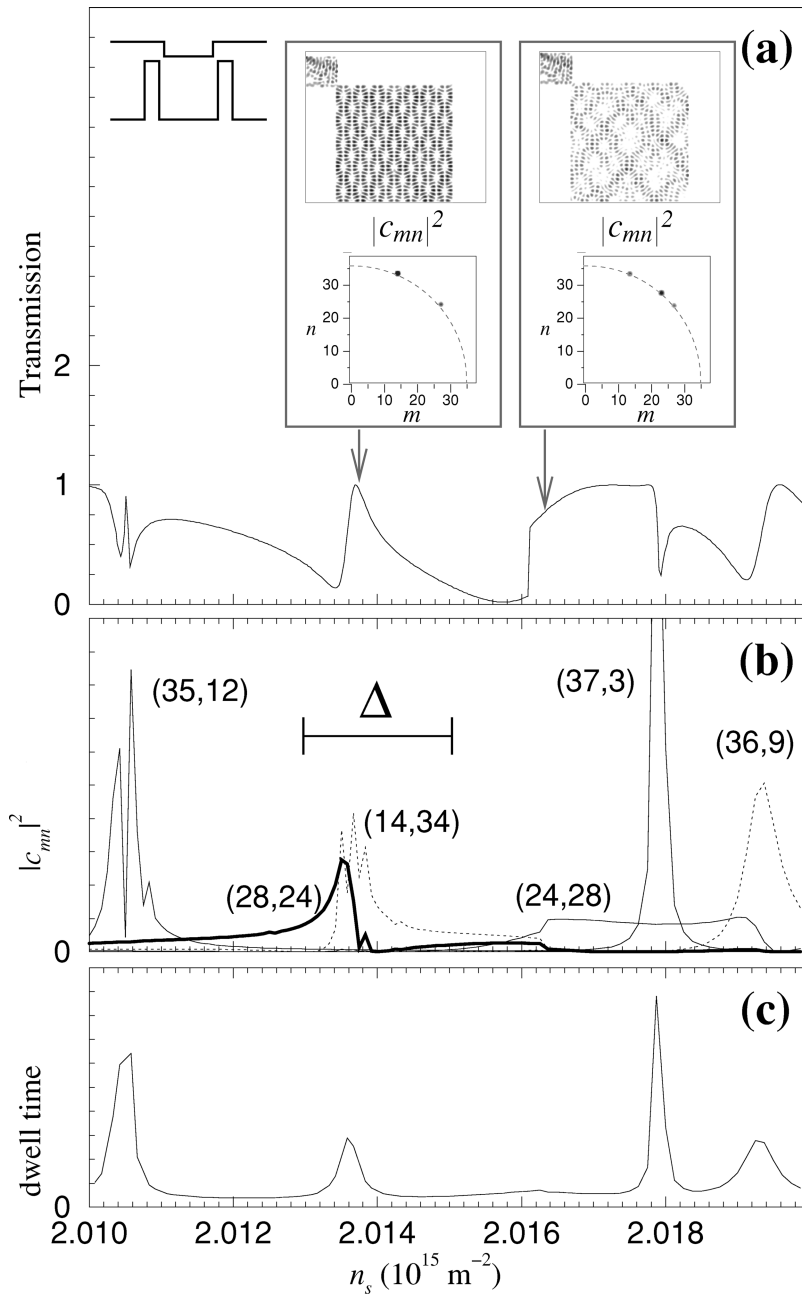


FIG. 2. (a) The conductance of the square dot (schematically depicted in the inset) as a function of the sheet electron density  $n_s = E_F m^* / \pi \hbar^2$ . The side of the dot  $L = 1 \mu\text{m}$ ; temperature  $T = 0$ . The lead openings support one propagating mode. Insets show calculated  $|\Psi(x, y)|^2$  inside the dot for two representative values of  $n_s$  and the corresponding numerical results for the coefficients  $|c_{mn}|^2$  calculated on the basis of Eq. (1). Dashed lines indicate the circle with the radius  $r = k_F L / \pi$ . (b) Dependence of the coefficients  $|c_{mn}|^2$  identifying the dominant resonant states with the quantum numbers  $(m, n)$  on the sheet electron density  $n_s$ . A horizontal bar indicates the mean energy level spacing  $\Delta$ . (c) Dwell time of the dot calculated numerically on the basis of Eq. (2).

square are not easily recognized. Thus, a numerical analysis on the basis of Eq. (1), in contrast to the tunneling case, is essential. Calculating the expansion coefficients  $c_{mn}$ , we find that, at the given  $k_F$ , only those coefficients associated with the circle in the  $k$  space with the radius  $R = k_F \approx \sqrt{2m^* \epsilon_{mn} / \hbar} = \pi \sqrt{m^2 + n^2} / L$  are distinct from zero, see Fig. 2(a). (Note that nonvanishing contributions from other coefficients would indicate that eigenstates of the isolated dot are essentially distorted by the lead openings such that a discussion of the transport in open structure in terms of eigenstates of the isolated dot does not make sense.) Typically, we find that only a few (and sometimes even a single) coefficients give a dominant contribution. A broadening of the resonant levels due to the effect of the dot openings in the  $k$  space is less than the distance between neighboring eigenstates whose quantum numbers differ by one,  $\Delta k = |k_n - k_{n \pm 1}| = |k_m - k_{m \pm 1}| = \pi / L$ . Therefore, we conclude that *despite the presence of dot openings, transport*

*through the structure is still effectively mediated by a few eigenstates of the corresponding closed dot with the eigenenergies lying in close proximity to the Fermi energy,  $\epsilon_{mn} \approx E_F$ .*

Calculating the coefficients  $c_{mn}$  as a function of the Fermi energy, we extract information about the lead-induced broadening of the energy levels of the dot. A contribution of the dominant resonant energy states is shown in Fig. 2(b) (at a given Fermi energy, remaining coefficients are at least of the order of magnitude smaller than those shown in the figure). The mean energy level spacing,  $\Delta = 2\pi \hbar^2 / m^* L^2 \sim 70 \text{ mK}$ , is indicated by a horizontal bar. In contrast to the tunneling regime, the line shape of  $|c_{mn}(E)|^2$  can be non-Lorentzian. Moreover, different states are characterized by different broadenings and they may overlap with each other. However, a broadening (half width) of the resonant energy levels is typically less than  $\Delta$ . Therefore, *transport measurements*

at very low temperatures in a single-mode regime in the leads may probe a single resonant energy level of the dot.

A comparison between Figs. 2(a) and 2(b) shows that features in the conductance of the dot are related to excitations of the particular eigenstates of the square. However, this correspondence is rather complicated: different eigenstates can be responsible for opposite features in the dot conductance. As an example, the eigenstate (14,34) causes a conductance peak, whereas the eigenstate (37,3) leads to a dip.

The above features in the conductance can be understood on the basis of a simple ‘‘resonant tunneling’’ model. If only one single eigenstate is excited in the dot at the given Fermi energy, it gives rise to a conduction peak, similar to that one in the tunneling regime (though much broadened due to the effect of the lead openings). If several eigenstates effectively mediate transport, interference between them may cause the amplitude of the total wave function in the vicinity of two dot openings to be different. This, in turn, will lead to a difference in coupling strengths between the state inside the dot and, correspondingly, incoming and outgoing states in the left and right leads. In this case ‘‘resonant’’ transmission with the unitary transmission coefficient is no longer possible. Therefore, in the case where several states simultaneously mediate transport in the dot, the phase relations between them and their mutual interference define the coupling strength to the outer states and govern the behavior of the transmission coefficient.

### C. Many-mode regime

Figure 3, left panel, shows a probability density distribution for one representative value of  $k_F$  in a square dot where lead openings transmit  $N=1,3,10$  propagating modes. The corresponding expansion coefficients  $c_{mn}$  calculated on the basis of Eq. (1) are shown in the right panel. As the lead openings become wider, a number of the resonant states excited in the dot increases. Nevertheless, like in the single-mode regime, at the given Fermi energy, a nonvanishing contribution comes only from the coefficients which lie in the closest proximity to the circle with the radius  $k_F$  in the  $k$  space. Therefore, even in a many-mode regime, transport through an open structure is still effectively mediated by eigenstates of the corresponding closed dot.

A broadening of the resonant energy levels increases with an increase of the lead openings. This is illustrated in Fig. 4 for a square dot where  $N=5$  propagating modes are available in the leads. Wave-function patterns are analyzed on the basis of Eq. (1) and contributions from dominant states are shown in a representative interval of the Fermi energy. Typically, several states dominate transport at a given  $E_F$ . A broadening of the energy levels has, as a rule, a complicated essentially non-Lorentzian character with half width being different for different states. In contrast to the single-mode regime, a half width of the resonant energy levels is typically larger than the mean energy level spacing,  $\Delta$ . It is interesting to note, however, that the broadening of some resonant states still does not exceed  $\Delta$  even with five modes in the leads. Comparing the conductance of the dot, Fig. 4 and the dependence  $c_{mn} = c_{mn}(E_F)$ , one can trace a certain correspondence between the two. However, because many eigenstates typi-

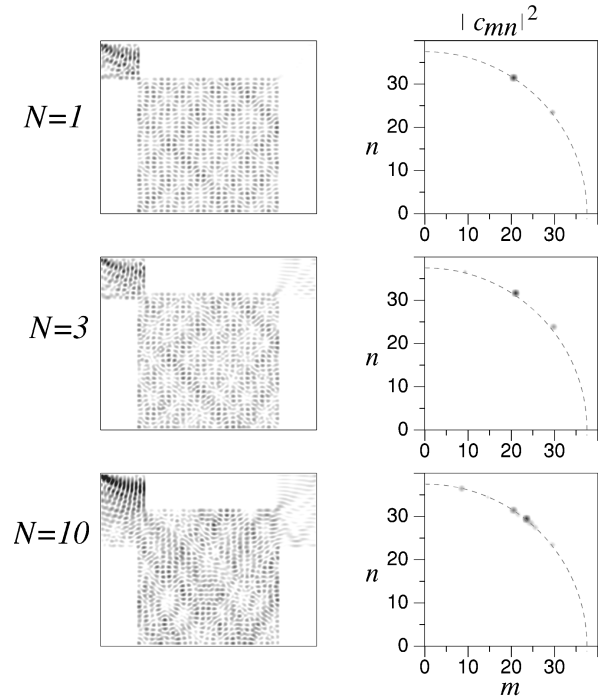


FIG. 3. Left panel: probability density distribution  $|\Psi(x,y)|^2$  for the dot of Fig. 2 calculated for one representative value of  $k_F = 1.15 \times 10^8 \text{ m}^{-1}$ . Dot openings support  $N=1,3,10$  modes (top to bottom). Right panel: corresponding expansion coefficients  $|c_{mn}|^2$  calculated on the basis of Eq. (1). Dashed lines indicate the circle with the radius  $r = k_F L / \pi$ .

cally contribute to the conductance at a given  $E_F$ , a detailed explanation of the features of the dot conductance is not possible.

### D. Wave-function scarring

A probability density distribution pattern has been visualized for a number of open structures, like stadium-shaped,<sup>18</sup> circular,<sup>18,24</sup> or square dots.<sup>10,41</sup> The density distribution of both chaotic and regular structures forms patterns or regions of enhanced density. In *closed* stadium billiards, for example, such regions, so-called scars, sometimes resemble classical trajectories in a striking way.<sup>27,42</sup> In analogy to this, the diamondlike features found in the wave function pattern in an open square dot have been associated with the classical trajectories of a particle bouncing in the square.<sup>10</sup> The natural question to be asked in this context is ‘‘Do scarred features in open dots represent a new ‘‘animal,’’ or can they be related to well-known ‘‘scarred’’ eigenstates of the classically chaotic closed systems?’’

The probability density distribution of the total wave function in the dot under consideration generally has a complicated character, see Figs. 2, 3. However, our expansion analysis, Eq. (1), unambiguously shows that the complex pattern observed is merely a result of a superposition of a few regular eigenstates of the square taken with different weights. Occasionally the pattern associated with  $|\Psi(x,y)|^2$  exhibits features resembling the classical ball trajectories in the square [right image in Fig. 2 (a)]. However, they can hardly be identified with them. Indeed, according to the Heisenberg principle, the uncertainty in spatial coordi-

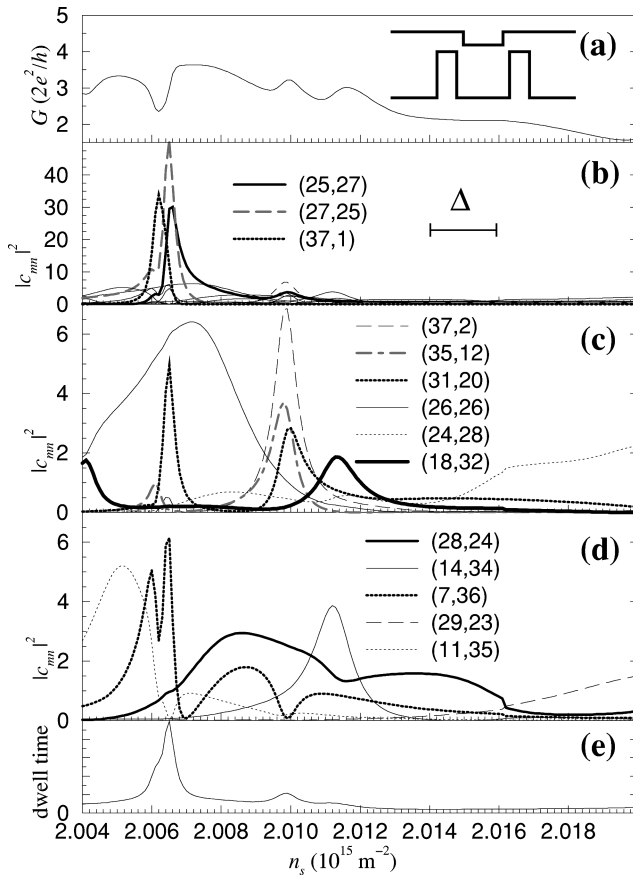


FIG. 4. (a) The conductance of the square dot (see inset) in a many-mode regime in the lead openings,  $N=5$ . The side of the dot  $L=1 \mu\text{m}$ ; temperature  $T=0$ . (b) Coefficients  $|c_{mn}|^2$  identifying the dominant resonant states with the quantum numbers  $(m,n)$ . A horizontal bar indicates the mean energy level spacing  $\Delta$ . (c), (d) The same as (b) but in a refined scale. [The contribution from the three dominant states indicated in (b) is not shown.] (e) Dwell time of the dot calculated on the basis of Eq. (2).

nate is  $\Delta x \sim 1/\Delta k$ . The uncertainty of the  $k$  vector of an electron in the dot is determined by the broadening of the resonant levels and, is shown in Sec. III B, to be of the order of  $\Delta k = \pi/L$ . This gives us  $\Delta x \sim L$ , indicating that an electron is delocalized in the dot and the above “scars” represent an interference picture of a few sine-type particle-in-the-box eigenstates.

Note that our analysis has been performed for the square dot where particle-in-the-box eigenstates can be written in a simple analytical form. However, we are confident that our major conclusion that transport in an open structure is effectively mediated by the eigenstates of the corresponding closed system holds regardless of the shape and underlying classical dynamics (regular or chaotic). In particular, total wave functions in an open circular dot calculated by Berggren *et al.*<sup>24</sup> show that transport through the dot occurs via states resembling corresponding Bessel-type wave functions for the isolated circle. Besides, it seems unlikely that a presence of the weak magnetic field could change a situation as far as the cyclotron radius is (much) larger than the dot size and the edge state regime is not achieved (i.e., adiabatic transport via edge states does not take place).

Therefore, we conclude that scarred features seen in the wave-function density distribution in a square dot are not related to classical trajectories, but can be thought of as a result of superposition and mutual interference of several regular eigenstates of the corresponding closed structure mediating transport at the given Fermi energy. (Occasionally they may resemble classical trajectories,<sup>10</sup> although scars in this sense are scarce.) Instead, we shall focus on a different aspect of the probability density pattern in the square dot. Namely, the features typically seen in the portraits of  $|\Psi(x,y)|^2$  in a striking way resemble “scarlets,” the random network of ridges resulting from the superposition of the plane waves with random amplitudes, directions, and phases but with the same wave-vector magnitude.<sup>43</sup> In contrast, a similar superposition of the plane waves but with the spread of wave-vector magnitude produces a qualitatively different, speckle-type pattern. The scarlets are thought to be the precursors of scars, since they are much less organized and are not directly related to the periodic orbits.<sup>44</sup> The above similarity is not accidental and is merely due to the fact that only states with the same wave vector (close to  $k_F$ ) are excited in the dot. Similar “scarlets” features have also been experimentally observed as a network of capillary waves formed on a water surface in agitated ripple tanks.<sup>38</sup> Note that in the latter case the behavior of the velocity potential of the water surface is governed by the Helmholtz equation which in a certain limit is equivalent to the two-dimensional stationary Schrödinger equation for a quantum particle.

#### E. Can one discuss transport characteristics of open dots on the basis of the eigenlevel spacing statistics of the corresponding isolated systems?

In this section we critically examine several approaches<sup>20,28</sup> to the analysis of the statistics of the spectra of open dots. On the basis of our direct mapping of resonant states performed for an open square dot, we hope to contribute to the clarification of some fundamental issues in this context.

A statistical analysis of the distribution of the energies at resonances of conduction fluctuations in chaotic stadium and regular circular billiards has been performed by Ishio.<sup>20</sup> In both billiards the statistics follow the Wigner-type distribution which was taken as an indication that “even a small perturbation around the holes (lead openings) immediately causes some nonintegrable effect on the statistics.” With regard to this analysis, the question immediately arises “does the resonance energy statistics of the conductance fluctuations reproduce the corresponding statistics of the isolated system?” In Sec. III B we have shown that features in the conductance oscillations can be understood from the analysis of the set of eigenstates mediating transport at the given Fermi energy. However, even in a single-mode regime, resonant energies in the conductance fluctuations only occasionally correspond to resonant eigenstates of the isolated dot. Instead, in most cases resonant energies are related to those energies when more than one state is simultaneously excited in the dot such that their mutual interference leads to the resonance behavior of the transmission coefficient. Therefore, in our opinion, Wigner-type statistics of the spacing of

the conductance fluctuation resonances cannot be taken as an indication of the transition to chaos in a nominally regular but open system.

Wang *et al.*<sup>28</sup> analyzed statistics of the open system on the basis of the calculated electron dwell time,

$$\tau = \int ds |\Psi(x,y)|^2 / j, \quad (2)$$

which identifies the time an electron spends inside the dot; in the above definition an integration is performed within the dot area and  $j$  is the incoming flux. Statistics of the spectra (which was assumed to be reproduced by a statistics of the dwell time maxima energies separations; see also<sup>45</sup> for a discussion of general relation between density of states and dwell times in mesoscopic systems) were found to be exactly the same as that of the corresponding closed system. Again, a similar question arises, ‘‘does the dwell time maxima (which is integrated characteristic) unambiguously identify individual resonant states of the open dot?’’

Figures 2(c) and Fig. 4(c) show the calculated dwell time in the square dot in the single- and many-mode regimes, respectively. In a single-mode regime all maxima in the dwell time do correspond to the resonant eigenstates, [cf. Figs. 2(b) and 2(c)], in contrast to the conduction fluctuation resonances. However, dwell time does not identify resonant states unambiguously because some eigenstates are overlooked by this analysis. For example, an eigenstate (24,28) which gives rise to a broad maximum in the conductance, does not contribute appreciably to the dwell time. In addition, some resonant levels cannot be resolved in the dwell time dependence. As an example, a single maximum of the dwell time just below  $n_s = 2.014 \times 10^{15} \text{ m}^{-2}$  represents a contribution of two eigenstates, (28,24) and (14,34).

Nevertheless, despite the fact that the dwell times do not unambiguously identify resonant states, our analysis, as far as a single mode regime is concerned, tends to support the conclusion<sup>28</sup> that the statistics of the dwell time spectra for open dots are the same as that of the corresponding closed systems. Indeed, it is important to stress that dwell time maxima are attributed to the resonant states only. (This is in contrast to the statistics of the conductance fluctuations where the majority of maxima are not directly related to the resonant eigenstates.) Suppose resonant state spacings form a statistical ensemble characterized by the Wigner (or Poisson) distribution. Obviously, dwell time maxima spacings represent a subensemble of the whole ensemble, since, as we have shown above, some of the resonant states have not shown up in the dwell time analysis. Since the number of missing states is small, however, one can expect that this subensemble is characterized by the same statistical distribution as the original one.

Let us now discuss a many mode regime of a transport through the dot. The calculated dwell time has two maxima in the interval of the Fermi energy represented in Fig. 4. At the same time, as many as 14 resonant states dominate the conductance in this energy interval. Most of these states, for example, (24,28), (11,35), (28,24), do not contribute to the dwell time maxima. The observed maxima in the dwell time are a result of overlapping of several eigenstates which are peaked near the same energy [like those depicted in Fig. 4(b)]. This leads us to conclude that in a many-mode regime

the dwell time does not properly identify resonant eigenstates mediating transport through the dot.

Furthermore, the results of our analysis strongly suggest that in a many-mode regime the resonant level spacing statistics become ill-defined. This is not only because the broadening of resonant states typically exceeds mean level spacing (for Lorentzian broadening one can still define statistics of the spacings between peak maxima). This is due to the fact that the broadening itself in many cases is essentially non-Lorentzian. Consider, for example, state (18,32), Fig. 4(c). Its energy dependence is characterized by two maxima of almost equal height, separated by a distance which several times exceeds  $\Delta$ . Several other states [(31,20), (28,24), (7,36)] are characterized by similar behavior. Some other states, like (24,28), dominate transport over the energy interval much greater than the mean level separation. At the same time its energy dependence shows broad features without any well-defined maximum. For the above mentioned states the concept of statistics of the spectra does not make any sense, since it is not possible to introduce any reasonable definition of the spacing between resonances. Therefore, we conclude that *for the quantum dots strongly coupled to the leads with several modes available in the lead openings, eigenlevel spacing statistics of the corresponding closed system are not relevant to the averaged transport properties of the structure.*

This conclusion seems to have a number of experimental as well as numerical verifications. The difference between statistical properties of the conductance oscillations in a chaotic (stadium) and a regular (circular) dots has been studied by Marcus *et al.*<sup>1</sup> Corresponding averaged autocorrelation functions are almost identical over the two decades of decay, although they exhibit quantitative distinctions in the tail. The data, from the similar studies of Berry *et al.*<sup>3</sup> for chaotic (circular with a bar) and regular (circular) dots, does not show any significant discrepancy over the four orders of magnitude in power. Note, that in the above mentioned experiments, the quantum-point-contact openings were adjusted to support three or more modes in order to meet the requirements of the semiclassical predictions<sup>14</sup> (which are, strictly speaking, valid for a large number of open channels in the leads). Numerical studies of autocorrelations functions have been performed by Wang *et al.*<sup>30</sup> for chaotic (stadium) and regular (circular) dots. They found, that in a weakly coupled regime, averaged autocorrelations functions behave differently, with a correlation function for a stadium-shaped dot satisfying predictions of the semiclassical theory. In contrast, in a strongly coupled regime, the difference between two sets of data is negligible, which is in accordance with our arguments.

We conclude this section by a brief discussion on the crossover between the single- and many-mode regime. Namely, about what number of open channels, lead-induced broadening of resonant levels becomes essentially non-Lorentzian such that the concept of spectra statistics loses its meaning. One can expect that in smaller dots where the mean level spacing is greater, the above crossover might occur for a larger number of modes,  $N$ , in leads. However, with the fixed width of the lead openings,  $w$ , the aspect ratio  $w/L$  is greater for smaller dots, which causes an opposite effect of increase of the level broadening. Having performed calcula-

tions for dots of different sizes, we did not find a universal recipe for the number of modes  $N$  at which such crossover occurs. Its value depends on a number of factors, such as the dot size, the aspect ratio  $w/L$ , and the Fermi energy of electrons. For the structure under consideration, non-Lorentzian broadening is dominant at  $N > 4 \sim 5$ .

## IV. CONDUCTANCE OSCILLATIONS

### A. The shell structure of the square dot

In the previous section we unambiguously showed that the conductance of the open dot is mediated by the resonant states of the corresponding closed structure. Before we proceed to the analysis of the calculated conductance it is instrumental to consider a simple ‘‘shell-structure model’’ introduced for the interpretation of the experiments on conduction fluctuations in the mesoscopic dots.<sup>6,23,24</sup>

A diagram illustrating the eigenspectrum of a square in the  $k$  space is shown in the inset of Fig. 5(a). The shaded band indicates a Fermi wave vector. A finite energy window is allowed for, in accordance with the above shell-structure model. All states within this finite window are assumed to contribute, with equal weight and broadening, to the conductance through the corresponding open dot.

The existence of at least two different shells is immediately anticipated. The first one corresponds to the case when  $k_F$  hits clustered states with one of the quantum numbers,  $n$  or  $m$  being close to one (and the second one is close to  $k_F L/\pi$ ). Such states are schematically indicated by the horizontal and vertical solid lines in the diagram. As  $k_F$  is varied, one repeatedly hits such states with the periodicity being defined by the distance between neighboring states,  $\Delta k L = \pi$ . Another shell corresponds to the clustering of the symmetric states,  $m \approx n$  (diagonal solid lines), separated by the distance  $\Delta k L = \pi/\sqrt{2}$ .

The Lorentzian broadened density of states of the square is shown in the inset of Fig. 5. Its Fourier transform reveals several pronounced peaks related to the formations of the shell structures. In particular, first and second peaks (with  $\Delta k L = \pi$  and  $\Delta k L = \pi/\sqrt{2}$ ) reflect a formation of the two shells discussed above. As a guide to the eye, the triangles in the figure indicate the values of  $k_F$  where one expects the maxima in the DOS related to the formation of the first shell,  $k_F = \pi m/L$ .

The density of states of the quantum systems is related to the underlying dynamics of the corresponding classical systems. In particular, for chaotic billiards, this relationship is given by the Gutzwiller trace formula,<sup>27</sup> which approximates the oscillating part of the density of states by the sum over all classical periodic orbits. This approach was extended to the case of integrable systems, where the role of isolated orbits is typically taken over by degenerate families of non-isolated orbits.<sup>46</sup> In a square dot each family of periodic orbits can be labeled by two indices (winding numbers),  $(i, j)$ , describing the number of collisions with the vertical and horizontal walls.<sup>47</sup> Figure 5(a) shows expected contributions from the different families of orbits estimated from the Bohr-Sommerfeld quantization rules. Each major peak in the shell structure corresponds to the contribution from a certain family of orbits. We note a striking similarity between the character of eigenstates defining the shell and the corresponding

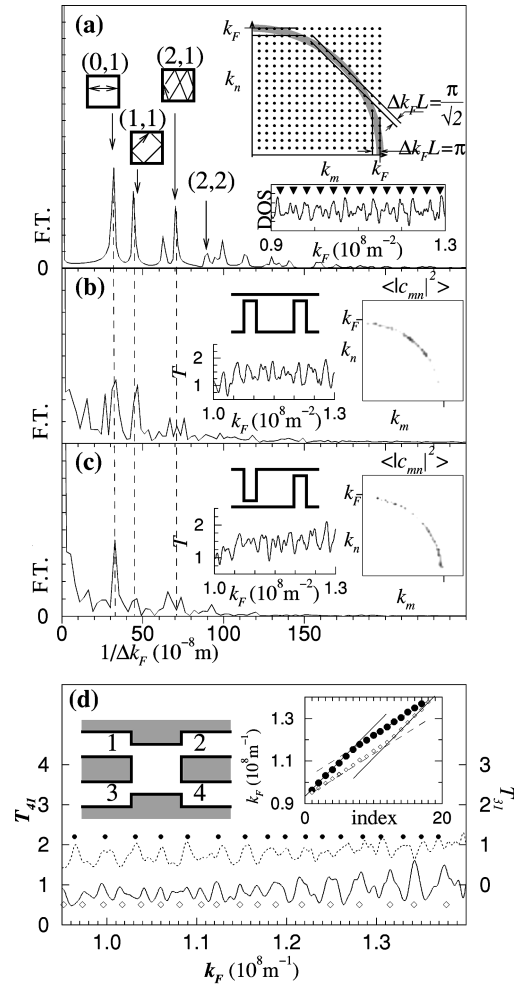


FIG. 5. (a) Upper right inset: A diagram illustrating the eigenspectrum of the square dot in the  $k$  space. Each point in the diagram represents an eigenvalue; the distance between the neighboring eigenvalues being  $\Delta k = \pi/L$ . Further explanations are given in the text. Lower right inset: density of states (DOS) of the square with the side  $L = 1 \mu\text{m}$  calculated for the Lorentzian broadening of the levels corresponding to the  $T = 500$  mK. Left: A Fourier transform of the DOS. Arrows show the expected contribution from the families of primitive periodic orbits which are schematically depicted in the figure. Numbers in the parenthesis indicate the winding numbers (see text). The first peak in the Fourier transform (F.T.) with  $1/\Delta k_F \approx 32 \times 10^{-8}$  m corresponds to the periodicity  $\Delta k_F L = \pi$ ; the second one with  $1/\Delta k_F \approx 44 \times 10^{-8}$  m corresponds to the periodicity  $\Delta k_F L = \pi/\sqrt{2}$ . (b), (c) A Fourier transform of the conductance fluctuations (lower left insets) of the square dot ( $L = 1 \mu\text{m}$ ) with different arrangements of the leads (upper left insets);  $T = 250$  mK. The right insets show averaged expansion coefficients  $\langle |c_{nm}|^2 \rangle$ . (d) Transmission coefficients  $T_{41}$  (solid lines) and  $T_{31}$  (dashed lines) for the square dot with  $L = 1 \mu\text{m}$  in the four-terminal geometry (inset);  $T = 250$  mK. Filled circles and open diamonds mark the transmission peaks. Solid lines on the index plot (right inset) correspond to the periodicity  $\Delta k_F L = \pi/\sqrt{2}$ , dashed lines correspond to  $\Delta k_F L = \pi$ .

classical orbits. For example, the family (0,1) corresponds to the ‘‘bouncing wall’’ orbits, where one of the components of the velocity,  $v_y$  (or  $v_x$ ) is zero. On the other hand, the corresponding shell, as discussed above, represents a contribution from the states for which  $k_n \approx 0$  (or  $k_m \approx 0$ ).



The second family of orbits with the winding numbers (1,1) represents electrons with equal components of velocities,  $|v_x|=|v_y|$ . The corresponding shell is formed by the symmetric states with  $k_m \approx k_n$ . Similar conclusions can be also drawn for other shells/families of orbits. In the next section we examine the manifestation of the shell structure of the square in the conductance oscillations of the corresponding open dot.

### B. Calculated conductance oscillations and their relation to the shell structure

Figure 5(b) shows conductance oscillations of the square dot where leads are placed opposite to each other as shown in the inset. The Fourier transform analysis reveals that all characteristic frequencies of the oscillations match those of the shell structure of the isolated square, cf. Figs. 5(a), 5(b). However, in addition to the frequencies associated with the formation of the shell structure, a new Fourier component ( $1/\Delta k_F \approx 15 \times 10^{-8}$  m, which corresponds to  $\Delta k_F L \approx 2\pi$ ) is present in the conductance of the open square. Its periodicity can be attributed to the nonclosed transversing trajectory connecting the two leads. Figure 5(c) shows conductance oscillations of the same dot of the square geometry but with the different arrangements of the leads which are now attached to the opposite corners (inset). Its Fourier transform reveals a striking difference to the previous case. In the present case one frequency,  $\Delta k_F L = \pi$ , is clearly dominant, indicating that only one selected set of eigenstates [corresponding to the family of orbits (0,1)] effectively mediate transport through the dot. To support this conclusion, we calculate the averaged expansion coefficients  $\langle |c_{mn}|^2 \rangle$ , see Figs. 5(b), 5(c), right insets (averaging is performed in the window in the  $k$  space which exceeds the largest characteristic periodicity in  $k_F$ ). The results of the calculations show that in the first case, Fig. 5(b), both symmetric states and states with  $\{k_m \approx 0, k_n \approx k_F\}$  are excited in the dot. However, in the second case, Fig. 5(c), when the leads are attached to the diagonally opposite corners, symmetric states with  $k_m \approx k_n$  are represented with much less weight. This is consistent with the observed suppression of the corresponding harmonics of conductance oscillations,  $\Delta k_F L = \pi/\sqrt{2}$ , which originates from the symmetric states of the isolated dot. Note that the above calculations have been performed for the case of  $N=3$  propagating modes in the constrictions connecting the dot to the leads. A detailed analysis of the conductance oscillations for the different  $N$  shows that all the features in the conductance associated with the shell structure of an isolated square are not sensitive to the number of modes in the constrictions.

In Ref. 12 the specific frequency of oscillations seen in the four-probe symmetric dot has also been attributed to the excitation of the particular set of eigenstates of the square. These selection rules were interpreted on the basis of the injection properties of the single QPC which directs an electron beam over the diagonal of the square due to the classical horn collimation effect. Our present analysis shows that the above injection alone cannot account for all the observed characteristics of the conductance. Namely, in both the quantum dots considered here all QPC's are identical. However, presumably due to a different coupling between entrance and

exit, contributions from some sets of the eigenstates (alternatively, families of periodic orbits) are suppressed. We do not have any convincing explanation concerning the particular selection rules which hold for a certain lead arrangement. On the contrary, consider the first dot with leads attached horizontally. One may expect that in this case a family of orbits (0,1), where electrons bounce between the opposite walls  $x=0,L$  would be dominant. However, the relative peak heights of the main frequencies of the conductance oscillations are the same as those of the shell structure of the isolated dot. This indicates that in this case the simple ‘‘shell-structure model’’ is a reasonable approximation which accounts for the major features of the oscillations for the geometry under consideration (excluding harmonics related to the traversing trajectories).

In the case of the second dot one would expect that two QPC openings placed over the diagonal of the square would be most effectively coupled by the the orbits belonging to the family (1,1). However, as we have found above, this contribution is strongly suppressed and, instead, orbits (0,1) are dominant. Thus, in this case the simple ‘‘shell-structure model’’ fails to predict a single characteristic frequency of the conductance oscillations.

Interpretation of the selection rules becomes even more difficult when several leads are attached to the dot. Figure 5(d) shows the transmission coefficients  $T_{41}$  and  $T_{21}$  for the dot in a four-terminal geometry depicted in the inset ( $T_{ij}$  is the transmission probability from the lead  $j$  to the lead  $i$ ). Arrows indicate the positions of the dominant peaks. One can clearly see a striking transition in periodicity of  $T_{41}$  ( $T_{21}$ ) at  $k_F \approx 1.2 \times 10^{15}$  m $^{-2}$ , when the characteristic frequency  $\Delta k_F L = \pi/\sqrt{2}$  ( $\Delta k_F L = \pi$ ) is taken over by the frequency  $\Delta k_F L = \pi$  ( $\Delta k_F L = \pi/\sqrt{2}$ ). This once again illustrates the observation that in the very same dot different sets of states (families of periodic orbits) effectively couple different leads in different energy windows.

In our calculations we did not account for an effect of inelastic scattering in the dot. Semi-classically, however, even if  $l_\phi \gg L$ , inelastic scattering suppresses a contribution from the long trajectories where electrons bounce in the dot for a long time. This effectively reduces high-frequency components of the fluctuations. Results<sup>12</sup> suggest that in a relatively large square dot (with the size of 2.4  $\mu$ m) only certain shells corresponding to the shortest orbits (or contributions from the transversing trajectories) dominate the conductance oscillations. One can expect that for dots of the size 1  $\mu$ m considered here, with the typical phase coherent length  $l_\phi \sim 5-10$   $\mu$ m, one can trace in the conductance fluctuations, contributions from the families of orbits up to (2,2) the length,  $l_{(2,2)} = 2L\sqrt{8}$ , of which does not exceed  $l_\phi$ .

To conclude this section we stress once again that the established correspondence between the conductance fluctuations and the Lorentzian broadened density of states holds regardless the particular shape of the dot. We have also performed calculations for a dot of triangular shape and found a one-to-one correspondence between the periodicity of the conductance oscillations of open triangular and the density of states of the corresponding isolated structure. These results, together with the related experiment, will be published elsewhere.<sup>48</sup>

## V. CONCLUSIONS

In this paper we study electron transport in an open square quantum dot with a size typical for current experiments. Our numerical analysis enables us to unambiguously identify the resonant states which dominate the conductance of the structure. On this basis we discuss various aspects of the electron transport through the dot.

The main results and findings of our work can be summarized as follows.

(i) Despite of the presence of dot openings, transport through the dot is effectively mediated by just a few eigenstates of the corresponding closed structure. This holds true even in the case of several propagating modes in the leads.

(ii) In a single-mode regime in the leads the broadening of the resonant levels is typically smaller than the mean energy level spacing,  $\Delta$ . Thus, at zero temperature, transport measurement in a single-mode regime may probe a single resonant energy level of the dot. On the contrary, in the many-mode regime the broadening exceeds  $\Delta$  and has essentially a non-Lorentzian character.

(iii) Transport characteristics of open dots (chaotic vs regular) are usually discussed on the basis of the statistics of the nearest level spacing of the corresponding closed system. As far as the single-mode regime is concerned, our results tend to support the conclusion that the statistics of the spectra for open dots follow those of the corresponding closed system. In the many-mode regime we argue that the concept of the statistics of the spectra does not make any sense, since it is not possible to introduce any reasonable definition of the spacings between resonances due to irregular character of the

broadening of resonant states. Thus we conclude that for the quantum dots strongly coupled to the leads, eigenlevel spacing statistics of the corresponding closed system are not relevant to the averaged transport properties of the structure. This conclusion seems to have a number of experimental as well as numerical verifications.

(iv) The density of states of the isolated square is characterized by the global shell-like structures which reflect periodic clustering of levels on the scale exceeding the mean level spacing separation. Each shell can be ascribed to the certain family of the periodic orbits in the square. There exists a striking correspondence between the character of eigenstates defining different shells and the corresponding families of orbits.

(v) The observed periodicity of the conduction oscillations in the open dots is related to the formation of the global shell structure of the corresponding isolated square. However, a particular arrangement of the leads may lead to the selective coupling between them, such that only selected shells (or, alternatively, families of periodic orbits) would dominate transport through the dot. These predictions can be experimentally tested in the two-terminal magnetoresistance measurement on the square dots with different arrangements of the leads.

## ACKNOWLEDGMENTS

We benefited from a fruitful interaction with K. Ensslin. We are grateful for a stimulating discussion with M. Gutzwiller. I.V.Z. acknowledges a grant from the Royal Swedish Academy of Sciences.

- 
- <sup>1</sup>C. M. Marcus, A. J. Rimberg, R. M. Westervelt, P. F. Hopkins, and A. C. Gossard, *Phys. Rev. Lett.* **69**, 506 (1992); C. M. Marcus, R. M. Westervelt, P. F. Hopkins, and A. C. Gossard, *CHAOS* **3**, 634 (1993).
- <sup>2</sup>M. J. Berry, J. A. Katine, C. M. Marcus, R. M. Westervelt, and A. C. Gossard, *Surf. Sci.* **305**, 495 (1994).
- <sup>3</sup>M. J. Berry, J. A. Katine, R. M. Westervelt, and A. C. Gossard, *Phys. Rev. B* **50**, 17 721 (1994).
- <sup>4</sup>A. M. Chang, H. U. Baranger, L. N. Pfeiffer, and K. W. West, *Phys. Rev. Lett.* **73**, 2111 (1994).
- <sup>5</sup>H. I. Chan, R. M. Clarke, C. M. Marcus, K. Campman, and A. C. Gossard, *Phys. Rev. Lett.* **74**, 3876 (1995).
- <sup>6</sup>M. Persson, J. Pettersson, B. von Sydow, P. E. Lindelof, A. Kristensen, and K.-F. Berggren, *Phys. Rev. B* **52**, 8921 (1995).
- <sup>7</sup>J. P. Bird, K. Ishibashi, D. K. Ferry, Y. Ochiai, Y. Aoyagi, and T. Sugano, *Phys. Rev. B* **52**, 8295 (1995).
- <sup>8</sup>J. P. Bird, D. M. Olatona, R. Newbury, R. P. Taylor, K. Ishibashi, M. Stopa, Y. Aoyagi, T. Sugano, and Y. Ochiai, *Phys. Rev. B* **53**, 14 336 (1995).
- <sup>9</sup>M. W. Keller, A. Mittal, J. W. Sleight, R. G. Wheeler, D. E. Prober, R. N. Sacks, and H. Shrtikmann, *Phys. Rev. B* **53**, R1 693 (1996).
- <sup>10</sup>R. Akis, D. K. Ferry, and J. P. Bird, *Phys. Rev. B* **54**, 17 705 (1996).
- <sup>11</sup>R. Schuster and K. Ensslin, in *The Physics of Semiconductors*, edited by M. Scheffler and R. Zimmermann (World Scientific, Singapore, 1996), Vol. 2, p. 1557.
- <sup>12</sup>I. V. Zozoulenko, R. Schuster, K.-F. Berggren, and K. Ensslin, *Jpn. J. Appl. Phys.* 1 (to be published); I. V. Zozoulenko, R. Schuster, K.-F. Berggren, and K. Ensslin, *Phys. Rev. B* **55**, R10 209 (1997).
- <sup>13</sup>R. Blümel and U. Smilansky, *Phys. Rev. Lett.* **60**, 477 (1988).
- <sup>14</sup>R. A. Jalabert, H. U. Baranger, and A. D. Stone, *Phys. Rev. Lett.* **65**, 2442 (1990).
- <sup>15</sup>R. V. Jensen, *CHAOS* **1**, 101 (1991).
- <sup>16</sup>H. U. Baranger, R. A. Jalabert, and A. D. Stone, *Phys. Rev. Lett.* **70**, 3876 (1993).
- <sup>17</sup>H. U. Baranger and P. A. Mello, *Phys. Rev. Lett.* **73**, 142 (1994); R. A. Jalabert, J.-L. Pichard, and C. W. J. Beenakker, *Europhys. Lett.* **27**, 255 (1994).
- <sup>18</sup>K. Nakamuro and H. Ishio, *J. Phys. Soc. Jpn.* **61**, 3939 (1992).
- <sup>19</sup>H. Ishio and J. Burgdöfger, *Phys. Rev. B* **51**, 2013 (1995); X. Yang, H. Ishio, and J. Burgdöfger, *ibid.* **52**, 8219 (1995).
- <sup>20</sup>H. Ishio, *J. Stat. Phys.* **83**, 203 (1996).
- <sup>21</sup>I. V. Zozoulenko and K.-F. Berggren, *Phys. Rev. B* **54**, 5823 (1996).
- <sup>22</sup>C. D. Schwilters, J. A. Alford, and J. B. Delos, *Phys. Rev. B* **54**, 10 652 (1996).
- <sup>23</sup>S. M. Reiman, M. Persson, P. E. Lindelof, and M. Brack, *Z. Phys. B* **101**, 377 (1996).
- <sup>24</sup>K.-F. Berggren, Z.-L. Ji, and T. Lundberg, *Phys. Rev. B* **54**, 11 612 (1996).

- <sup>25</sup>D. Weiss, K. Richter, A. Mensching, R. Bergmann, H. Schweizer, K. von Klitzing, and G. Weimann, *Phys. Rev. Lett.* **70**, 4118 (1993); H. Silberbauer and U. Rössler, *Phys. Rev. B* **50**, 11 911 (1994); G. Hackenbroich and F. von Oppen, *Europhys. Lett.* **29**, 151 (1995); S. Ishizaka, F. Nihey, K. Nakamura, J. Sone, and T. Ando, *Phys. Rev. B* **51**, 9881 (1995); I. V. Zozoulenko, F. A. Maaø, and E. H. Hauge, *ibid.* **53**, 7987 (1996).
- <sup>26</sup>J. Pedersen, S. Bjørnholm, J. Borggreen, K. Hansen, T. P. Martin, and H. D. Rasmussen, *Nature (London)* **353**, 733 (1991).
- <sup>27</sup>M. C. Gutzwiller, *Chaos in Classical and Quantum Mechanics* (Springer-Verlag, New York, 1991).
- <sup>28</sup>Y. Wang, N. Zhu, J. Wang, and H. Guo, *Phys. Rev. B* **53**, 16 408 (1996).
- <sup>29</sup>K.-F. Berggren and Z.-L. Ji, *CHAOS* **6**, 543 (1996).
- <sup>30</sup>Y. Wang, J. Wang, H. Gou, and C. Roland, *J. Phys.: Condens. Matter* **6**, L143 (1994).
- <sup>31</sup>In our calculations the reservoirs are represented by sufficiently wide channels of a constant width, supporting 30–50 propagating modes.
- <sup>32</sup>M. Macucci, K. Hess, and G. J. Iafrate, *J. Appl. Phys.* **77**, 3267 (1995).
- <sup>33</sup>Z.-L. Ji and K. F. Berggren, *Phys. Rev. B* **52**, R11 607 (1995).
- <sup>34</sup>K. Richter, D. Ullmo, and R. A. Jalabert, *Phys. Rev. B* **54**, R5 219 (1996).
- <sup>35</sup>C. W. J. Beenakker and H. van Houten, in *Solid State Physics: Advances in Research and Applications* (Academic, San Diego, 1991), Vol. 44; S. Datta, *Electronic Transport in Mesoscopic Systems* (Cambridge University Press, Cambridge, 1995).
- <sup>36</sup>I. V. Zozoulenko, F. A. Maaø, and E. H. Hauge, *Phys. Rev. B* **53**, 7975 (1996); **53**, 7987 (1996); F. A. Maaø, I. V. Zozoulenko, and E. H. Hauge, *ibid.* **50**, 17 320 (1994).
- <sup>37</sup>I. V. Zozoulenko, F. A. Maaø, and E. H. Hauge (unpublished).
- <sup>38</sup>R. Blümel, I. H. Davidson, W. P. Reinhardt, H. Lin, and M. Sharnoff, *Phys. Rev. A* **45**, 2641 (1992).
- <sup>39</sup>P. J. Price, *Phys. Rev. B* **38**, 1994 (1988).
- <sup>40</sup>J. Wang, Y. Wang, and H. Guo, *Appl. Phys. Lett.* **65**, 1793 (1994).
- <sup>41</sup>I. V. Zozoulenko and K. F. Berggren, *Phys. Scr.* **T69**, 345 (1997).
- <sup>42</sup>E. J. Heller, *Phys. Rev. Lett.* **53**, 1515 (1984).
- <sup>43</sup>P. O'Connor, J. Gehlen, and E. J. Heller, *Phys. Rev. Lett.* **58**, 1296 (1987).
- <sup>44</sup>E. J. Heller, in *Chaos and Quantum Physics*, 1989 Les Houches Lecture Notes (North-Holland, Amsterdam, 1991).
- <sup>45</sup>G. Iannaccone, *Phys. Rev. B* **51**, 4727 (1995).
- <sup>46</sup>V. M. Strutinsky and A. G. Magner, *Sov. J. Part. Nucl.* **7**, 138 (1976).
- <sup>47</sup>F. von Oppen, *Phys. Rev. B* **50**, 17 151 (1994).
- <sup>48</sup>H. Linke, L. Christensson, P. Omling, I. V. Zozoulenko, and K.-F. Berggren (unpublished).